

# Development of *in situ* gel containing CUR:HP- $\beta$ -CD inclusion complex prepared for ocular diseases: Formulation, characterization, anti-inflammatory, anti-oxidant evaluation and comprehensive release kinetic studies

Sedat ÜNAL <sup>1\*</sup> , Heybet Kerem POLAT <sup>2,3</sup> , Dönay YUVALI <sup>4</sup> , Esra KÖNGÜL ŞAFAK <sup>5</sup> 

<sup>1</sup> Department of Pharmaceutical Technology, Faculty of Pharmacy, Erciyes University, Kayseri, Türkiye.

<sup>2</sup> Department of Pharmaceutical Technology, Faculty of Pharmacy, Erzincan Binali YILDIRIM University, Erzincan, Türkiye.

<sup>3</sup> Turkish Medicines and Medical Devices Agency, Republic of Türkiye Ministry of Health, Ankara, Türkiye.

<sup>4</sup> Department of Analytical Chemistry, Faculty of Pharmacy, Erciyes University, Kayseri, Türkiye.

<sup>5</sup> Department of Pharmacognosy, Faculty of Pharmacy, Erciyes University, Kayseri, Türkiye.

\* Corresponding Author. E-mail: [sedatunal@erciyes.edu.tr](mailto:sedatunal@erciyes.edu.tr) (S.Ü.); Tel. +90-505-554 67 70.

Received: 05 August 2022 / Revised: 19 September 2022 / Accepted: 19 September 2022

**ABSTRACT:** In this study, cyclodextrin (HP- $\beta$ -CD) inclusion complexes were prepared with Curcumin (CUR) by cosolvency/lyophilization method. Characterization studies were performed with phase-solubility diagrams, scanning electron microscopy (SEM), FT-IR, FT-Raman, XRD, Differential scanning calorimetry (DSC). The prepared CUR:HP- $\beta$ -CD complexes were evaluated for their anti-oxidant and anti-inflammatory activities compared to free CUR and significantly higher activity was detected with the complexation. In addition, pre-formulation studies have been completed in order to develop an *in situ* gel formulation, containing CUR:HP- $\beta$ -CD, suitable for use in ocular diseases. To prepare the *in situ* forming gels, different Pluronic F127 (PF127) concentrations were used. Chitosan was added to the formulations to improve the gel's mucoadhesive properties. The formulations were evaluated for their viscosity pH, clarity, and sol-gel transition temperature. It was established that the formulations were all clear, their pH was 6, their gelation temperature decreased with increasing PF127, and was between 26-35 °C. Viscosities of all formulations were found to be suitable for ocular application. For the selected formulation, CUR and CUR:HP- $\beta$ -CD were loaded to *in situ* gelling systems. *In vitro* release experiments revealed that the CUR:HP- $\beta$ -CD inclusion complex including NSL formulation released for 6 hours with a higher burst effect than the other formulation. At the end of the study, *in situ* gel formulations containing CUR:HP- $\beta$ -CD were successfully prepared and characterized comprehensively. In addition, a detailed release kinetic study was conducted for the formulations and it was determined that the CUR release from the *in situ* gel formulations was compatible with the Weibull model. In conclusion, a mucoadhesive *in situ* gel formulation containing anti-oxidant and anti-inflammatory CUR:HP- $\beta$ -CD complex for ocular diseases is presented as an innovative formulation approach.

**KEYWORDS:** Curcumin; HP- $\beta$ -CD; release kinetics; ocular diseases; anti-inflammatory; anti-oxidant.

## 1. INTRODUCTION

Most (almost 90%) of ocular diseases are treated by topical administration of drug solutions (i.e., eye drops), especially in the anterior part of the eye. Topical instillation is the most practical route for ocular drug delivery. However, poor ocular bioavailability (5%) prevents this approach. The extremely impermeable anterior ocular surface is protected primarily by static barriers, such as the tight junctions of the conjunctiva and the alternating hydrophobic and hydrophilic corneal stroma, and by dynamic barriers, such as rapid tear turnover and the vasculature and lymphatics of the conjunctiva (1, 2). Innovative

**How to cite this article:** Ünal S, Polat HK, Yuvalı D, Köngül Şafak E. Development of *in situ* gel containing CUR:HP- $\beta$ -CD inclusion complex prepared for ocular diseases: Formulation, characterization, anti-inflammatory, anti-oxidant evaluation and comprehensive release kinetic studies. J Res Pharm. 2023; 27(1): 97-119.

formulation approaches, including hydrogels, polymeric micelles, nanosuspensions, and lipid-based nanocarriers, have been used to enhance ocular bioavailability during topical instillation (3, 4).

*In situ* gel drug delivery systems have become popular in recent years and are now utilized extensively in ophthalmic formulations. *In situ* gels are prepared using particular polymers that go through a sol-gel phase transition when exposed to environmental factors like pH (5), certain ions (6), and temperature (7). To promote patient compliance, *in situ* gel formulations are first made as solutions or suspensions, then transformed into gel when applied (8). For *in situ* gel formulations designed for application to the eye, various polymers or polymeric combinations can be used to prolong/modify the release profile as needed (9).

Pluronics, also known as poloxamers with a thermoresponsive structure, is one of the polymers widely used in the preparation of *in situ* gel systems. Due to the hydrophilic ethylene oxide portion and hydrophobic propylene oxide area, it displays amphiphilic behavior. The variation observed in the micelle structure with temperature and concentration is the basic principle of gelation of poloxamers. Since poloxamer *in situ* gel systems may prolong drug release and had inert character for the eye, poloxamers have been widely used as an ophthalmic drug delivery technology. However, the main drawback of poloxamer is its lack of adhesive properties for mucosal surfaces. Therefore, mucoadhesive polymers, such as sodium hyaluronate, carbopol, and chitosan (CH), have been utilized to improve the mucoadhesive properties of the poloxamer-based ocular formulations. With its cationic, biocompatible and biodegradable structure, CH can be used as an effective and promising polymer in ocular formulations. In addition, its advantages in the development of ocular formulations are noted with its strong mucoadhesive and also antimicrobial effects (10).

The yellow bioactive component of the perennial plant *Curcuma longa* L., known as curcumin (CUR), has a variety of physiological and pharmacological effects, including those that are anti-inflammatory, antioxidant, anti-cancer and neuroprotective (11). CUR has been shown to be effective when used topically for a variety of eye disorders and in this context protects retinal cells, retinal ganglion cells, and corneal epithelial cells while preventing the growth of human lens epithelial cells (12) at the same time CUR has been used to treat corneal and choroidal neovascularization (13, 14). Due to specific limitations such poor solubility, instability and poor absorption, CUR's therapeutic use in ophthalmology is restricted (15).

Innovative formulation approaches can be developed in order to overcome the pharmaceutical barriers associated with the active substance and resulting in clinical failure. In this context, pharmaceutical formulation trends such as polymers, carrier systems and new drug delivery systems come to the fore. With the developed formulations, solubility, stability and bioavailability problems of the therapeutic molecule can be eliminated and therapeutic efficacy can be achieved with a dosage form. The approach of solubilizing hydrophobic molecules by supramolecular complexation and increasing bioavailability is widely applied in the pharmaceutical field (16). Natural cyclic oligosaccharide polymers known as cyclodextrins (CD) are produced by the enzymatic breakdown of starch by the glucosyltransferase. The surface structure of CDs, which are described as having a cone-like three-dimensional shape, is hydrophilic while the inside cavity is hydrophobic; this facilitates the development of water-soluble complexes, including those containing medicines whose apolar cavities have poor water solubility (17). Therefore, by forming a drug-CD inclusion complex, the drug molecule can be protected from enzymatic or hydrolytic inactivation in the physiological environment, increasing bioavailability as a result of improved stability and solubility (18). As in many areas, CD can be used in the ocular area to increase the solubility of molecules with poor water solubility and to increase their corneal permeability. In the literature, there are studies in which various CD derivatives and CUR complexes are prepared for different indications and different administration routes. Hydroxypropyl-beta-cyclodextrin (HP- $\beta$ -CD) derivative obtained by superficial modification of beta-cyclodextrin ( $\beta$ -CD), a natural cyclodextrin, is widely used. When the literature is examined, high complexation efficiency and high solubility increase have been reported in studies in which HP- $\beta$ -CD CUR complex is formed, and it is considered as the main reason that many studies in this field shed light on future studies (19). Therefore, for the development of innovative formulations for ocular use, CD derivatives and drug-CD complexation approaches can be used to increase ocular bioavailability by increasing drug solubility and corneal penetration (20).

The main objective of this study is to prepare soluble and stable CUR:HP- $\beta$ -CD complexes embedded in heat-sensitive *in situ* gel formulations for ocular application and to comprehensively characterize the prepared formulations *in vitro*. For this purpose, an HP- $\beta$ -CD derivative was used as a complexing agent, and the complexes were prepared based on the data obtained at the end of the phase dissolution studies. Morphological properties (SEM), FT-IR, FT-Raman, XRD, DSC analyses of the prepared CUR:HP- $\beta$ -CD

complexes were performed. The anti-inflammatory and antioxidant activities were also analyzed. A heat-sensitive *in situ* gel formulation containing CH and PF-127 was then prepared. While CH is the formulation component benefiting from its mucoadhesive and antibacterial properties, PF-127 is used as the base gel polymer. The *in situ* prepared gel formulations were characterized in terms of their rheological properties, pH, clarity and gelling temperature. In addition, the *in vitro* release profiles of CUR from the *in situ* gel formulation were investigated in detail by mathematical modeling and the kinetics of CUR release were elucidated.

## 2. RESULTS

### 2.1. Characterization of CUR:HP-β-CD inclusion complex

#### 2.1.1. Phase-solubility and stability of CUR:HP-β-CD complex

Phase solubility studies not only provide information about the complexation stoichiometry of drug-CD inclusion complexes, but also provide information about the stability constant and stability of the inclusion complexes. To assess the impact of drug-CD complexation on drug solubility, phase-solubility tests are typically the method of choice (21). When a drug molecule is integrated into a CD molecule's cavity, the most common kind of association is the 1:1 drug/CD inclusion complex, which has a stability constant of K1:1 for the equilibrium between free and associated species. As seen in Figure 1, it was determined that the CUR solubility increased as a function of HP-β-CD concentration according to the phase-solubility diagram. According to the phase-solubility diagram, CUR:HP-β-CD diagram is classified as "AL-type" ( $r^2=0.9669$ ) (Figure 1), The slope was calculated to be 0.051. Complexation efficiency (CE) and stability constant (Ks) of CUR:HP-β-CD complex were calculated as 0.053 and 2933 M<sup>-1</sup>, respectively. In accordance with the literature, a Ks value of 100 to 10,000 M<sup>-1</sup> is suitable for stable complexation the drug:CD complex (22).

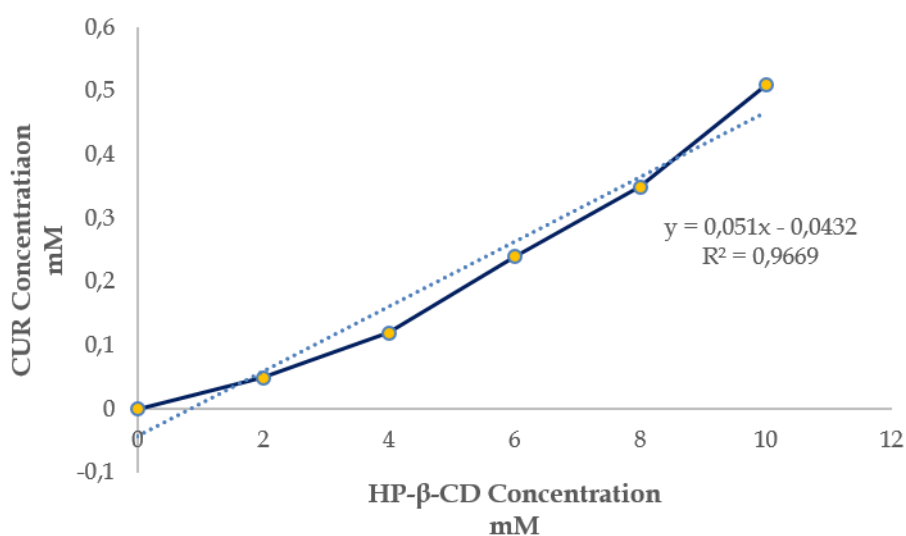


**Figure 1.** Phase-solubility diagram of CUR:HP-β-CD

#### 2.1.2. Complexation yield and solubility of CUR-HP-β-CD

The complexation yield of CUR:HP-β-CD inclusion complexes prepared according to the ethanol/water cosolvency/lyophilization method, as described in section 4.2., was calculated as 65.2%. In order to examine the water solubility of CUR and CUR:HP-β-CD, calculations were made by preparing their saturated solutions. It was already known that the solubility of CUR in water is very limited, at the end of the calculations it was found to be about 5.41 μg/mL, but for the CUR:HP-β-CD complex it was found that the solubility increased to 18.1 mg/mL and a clear solution could be obtained. Practically, the soluble CUR formulation was successfully achieved by the HP-β-CD complexing method.

### 2.1.3. Morphological analysis by scanning electron microscopy (SEM)

SEM images of pure CUR, HP- $\beta$ -CD, CUR:HP- $\beta$ -cyclodextrin inclusion complex and physical mixture of CUR/HP- $\beta$ -CD were obtained in order to examine the surface morphological properties in the characterization of the prepared inclusion complexes. SEM micrographs are presented in Figure 2. The pure CUR has an irregular crystal structure as seen in Figure 2A. In Figure 2B, it was seen that HP- $\beta$ -CD had a porous and rounded structure by contrast with CUR. Leafy scale-like SEM images in Figure 2C., differ from the morphology of the pure components. This structural difference confirms the formation of inclusion complexes between CUR and HP- $\beta$ -CD when compared with the SEM image of the physical mixture in Figure 2D. The results of SEM examination were considered to be consistent with previous studies (23).

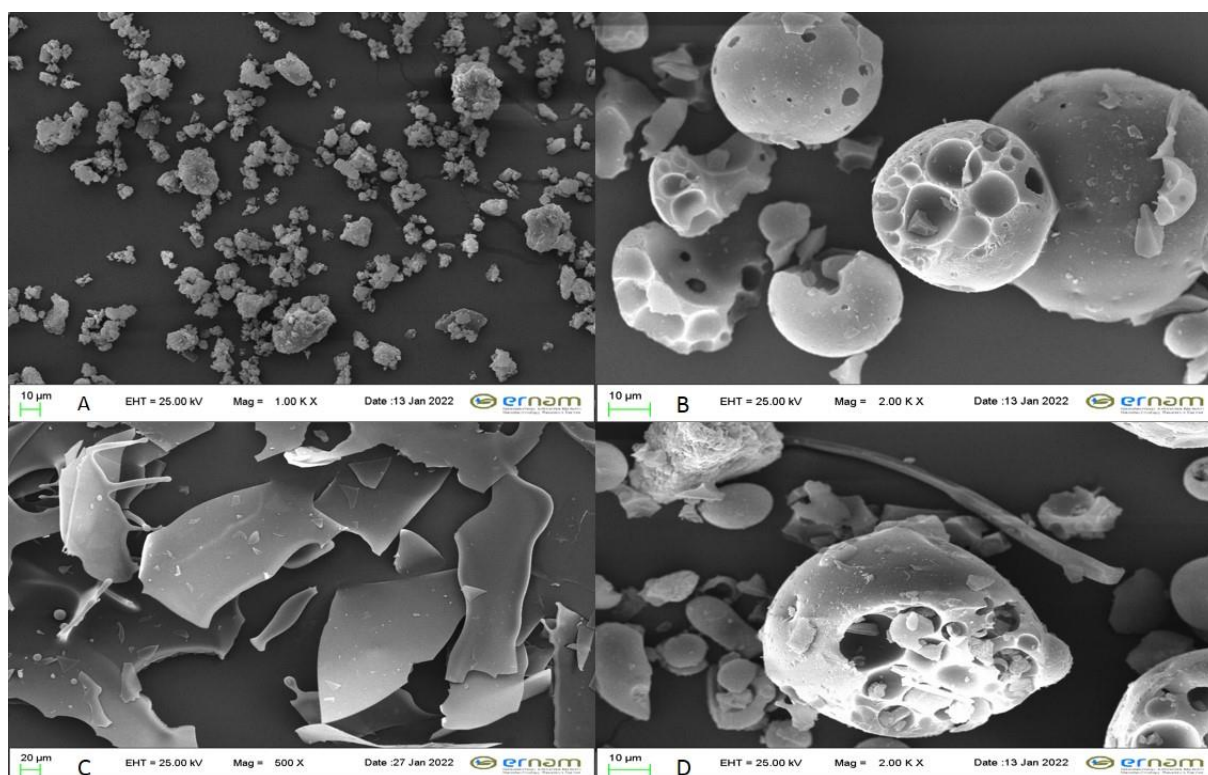


**Figure 2.** SEM images of CUR (A); HP- $\beta$ -CD (B); CUR:HP- $\beta$ -CD inclusion complex (C); CUR and HP- $\beta$ -CD physical mixture (D).

### 2.1.4. FT-IR analysis

FT-IR spectroscopy was used to detect the formation of the CUR inclusion complex. The FT-IR spectra of CUR, HP- $\beta$ -CD, CUR:HP- $\beta$ -CD inclusion complex and their physical mixture were presented in Figure 3. The IR spectrum of pure CUR was agreement with literature which is shown in Figure 3A. The three peaks at 3396, 3270 and 2974  $\text{cm}^{-1}$  in spectrum of CUR remarked the presence of OH group. The stretching vibrations of aromatic rings of CUR were seen at 1626  $\text{cm}^{-1}$  and another strong peak at 1586  $\text{cm}^{-1}$  that (C=C) and  $\nu(\text{C}=\text{O})$  vibration character.

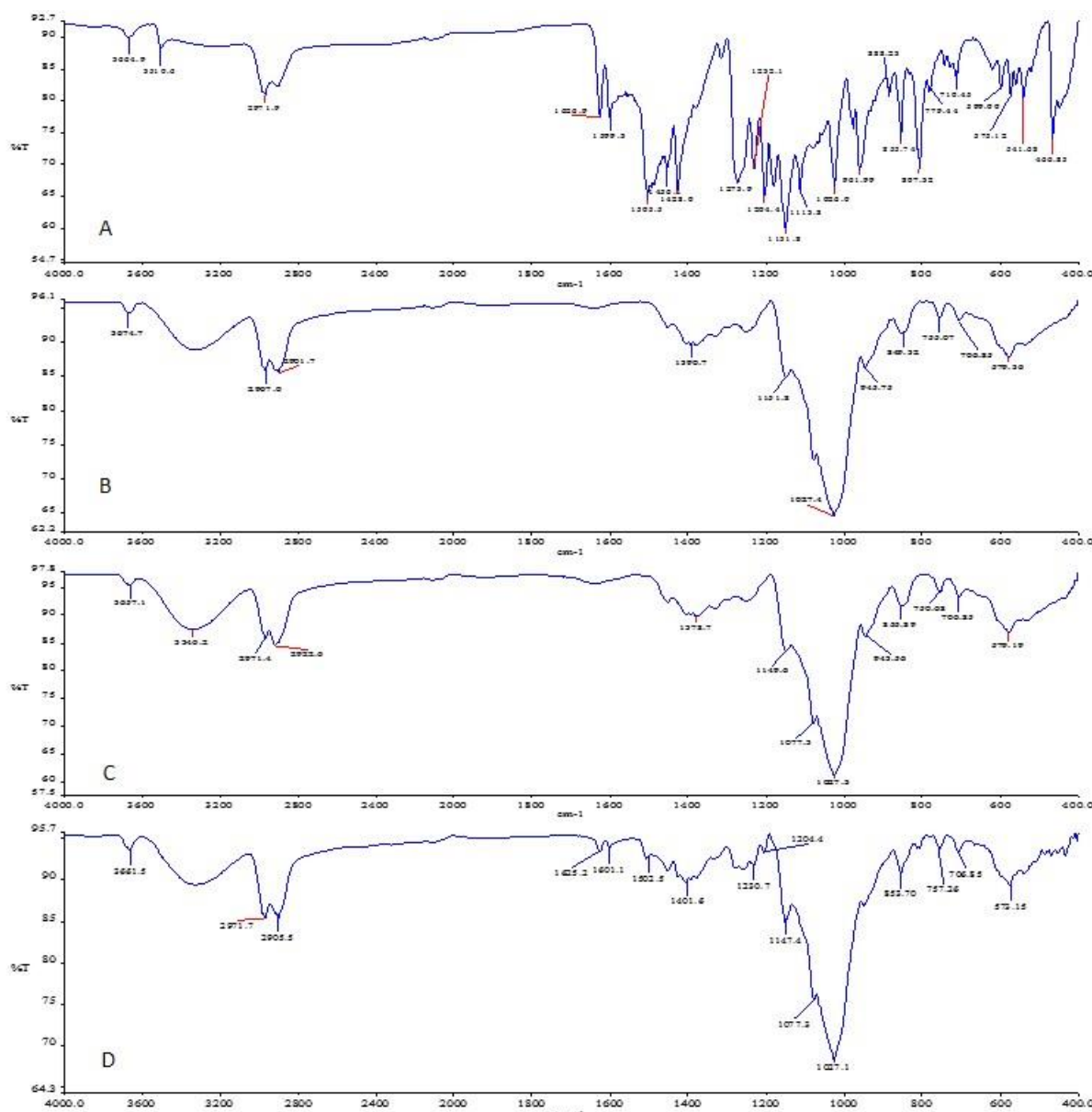


**Figure 3.** FT-IR spectra of CUR (A); HP-β-CD (B); CUR:HP-β-CD inclusion complex (C); CUR and HP-β-CD physical mixture (D).

In Figure 3B, FT-IR spectrum HP-β-CD show the characteristic OH group stretching vibrations at 3300-3400  $\text{cm}^{-1}$ . An intense peak at 2922  $\text{cm}^{-1}$  and 2924  $\text{cm}^{-1}$  due to C-H assym/symm stretching was seen HP-β-CD. The characteristic peak observed at 1033  $\text{cm}^{-1}$  is indicated to stretching vibration of C-O-C (24). As expected, the IR spectra of the CUR:HP-β-CD inclusion complex and physical mixture contained peaks corresponding to both the CUR and HP-β-CD. The complex and physical mixture did not demonstrate significant spectral differences due to low CUR extent and to the high absorption of HP-β-CD. The absorption peak of HP-β-CD can be seen, nevertheless characteristic peaks of CUR disappear. Due to the high intensity of the characteristic peaks of CD, the characteristic peaks of CUR disappear. It was determined that the analysis results of the FT-IR spectra were compatible with the CUR and HP-β-CD inclusion complex studies reported in the literature (25).

#### 2.1.5. FT-Raman

Raman spectra of components and complex, by FT-IR analysis, facilitate the assessment of inclusion complex formation. The Raman spectra of CUR, HP-β-CD, CUR:HP-β-CD inclusion complex and their physical mixture are shown in Figure 4. The intense G band at 1600  $\text{cm}^{-1}$ , resulting from aromatic ring vibrations (C=C ring) in the raman spectrum of pure CUR, was chosen to study the inclusion complex formation of CUR with cyclodextrin derivatives. In addition, two distinct peaks, a D band at 1150 and 1250

$\text{cm}^{-1}$ , were observed in the CUR raman spectrum given in Figure 4A. These intense peaks are due to vibrations of the C-H bond of the aromatic ring. Due to the chemical structure of HP- $\beta$ -CD, any peak is missed at G band in the raman spectrum which is shown in Figure 4B, besides, the peaks at D band are weak intensity. Although the simple mixture spectrum is expected to be the sum of the CUR and HP- $\beta$ -CD spectra, the obtained spectrum is the same as the raman spectrum of CUR (24).

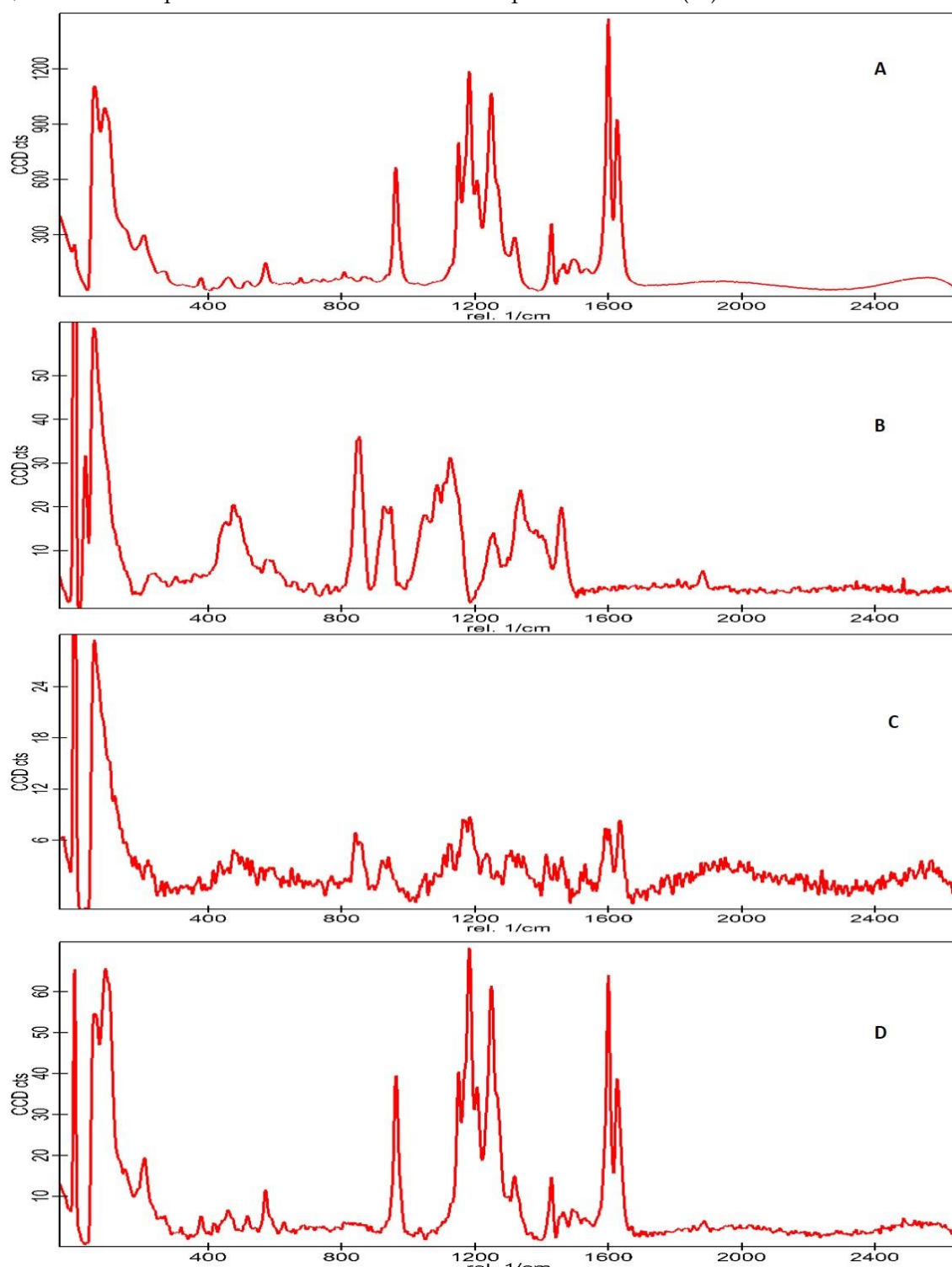


**Figure 4.** Raman spectra of CUR (A); HP- $\beta$ -CD (B); CUR:HP- $\beta$ -CD inclusion complex (C); CUR and HP- $\beta$ -CD physical mixture (D).

By comparing the Raman spectrum of the CUR:HP- $\beta$ -CD inclusion complex with the spectrum of the physical mixture, it is seen that the intensity of the peaks seen in the G and D bands decreases. The reasons for this decrease are thought one or both of the aromatic rings of CUR to be inside HP- $\beta$ -CD cavity (26).

### 2.1.6. XRD analysis

Powder X-ray diffraction analyzes were used to distinguish between crystalline and amorphous material and to explain the physical properties of the synthesized complexes. X-ray diffractograms of pure CUR, HP- $\beta$ -CD, CUR:HP- $\beta$ -CD inclusion complex, CUR and HP- $\beta$ -CD physical mixture are presented in Figure 5. The sharp and intense peaks that is diffraction angle of  $2\theta$  8.75, 14.9, 17.22, 21.05, 25.02 in the X-ray diffraction graph of pure CUR indicate that it is a crystalline form (27).

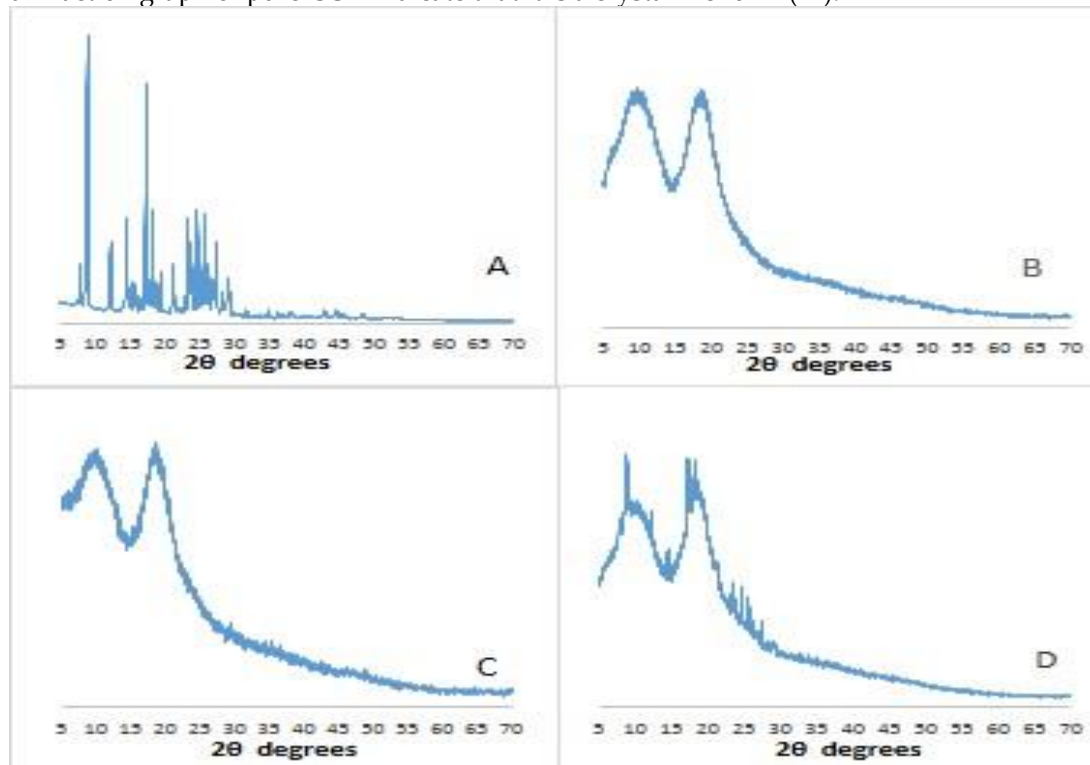


**Figure 5.** XRD analysis of CUR (A); HP- $\beta$ -CD (B); CUR:HP- $\beta$ -CD inclusion complex (C); CUR and HP- $\beta$ -CD physical mixture (D).

The XRD pattern of HP- $\beta$ -CD has characteristic two broad peaks in the ranges of 10–15 and 15–20 ( $2\theta$ ), in fact that has not sharp peaks, confirms its amorphous feature in nature (28).

The XRD of the physical mixture (presented in Figure 5D.) defined that the individual X-ray diffractograms of both CUR and HP- $\beta$ -CD overlapped approximately. It was observed that the XRD pattern of the inclusion complex was different from the XRD of the physical mixture and pure CUR, also similar to the XRD pattern of HP- $\beta$ -CD. The disappearance or decrease of the specific sharp peaks of CUR indicates the change in physical structure as a result of complex formation. The obtained SEM images, FT-IR spectra, Raman spectra and XRD patterns support each other and complex formation (29).

### 2.1.7. Differential scanning calorimetry (DSC) analysis

DSC is a characterization method used to explain the physical-chemical states of complexes synthesized from at least two different pure components. The complex formation may cause the disappearance or shift of the endothermic peaks of the active substance.

DSC thermograms of CUR, HP- $\beta$ -CD, their physical mixture and CUR:HP- $\beta$ -CD inclusion complex presented in Figure 6. CUR has a sharp endothermic peak at 180°C, corresponding to the melting point (Figure 6A) (27). Thermogram of HP- $\beta$ -CD (Figure 6B) shows a broad peak at 90–130°C due to loss of water. The thermal profile of their physical mixture was apparently a combination of characteristics of CUR and CD (Figure 6D).

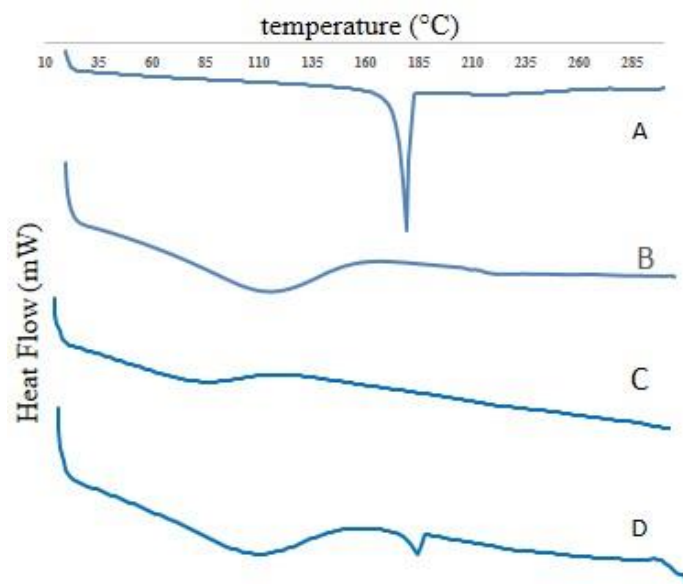


**Figure 6.** DSC thermograms of CUR (A); HP-β-CD (B); CUR:HP-β-CD inclusion complex (C); CUR and HP-β-CD physical mixture (D).

According to result of DSC curve of the CUR:HP-β-CD inclusion complex (Figure 6C.), it was observed that it was quite similar to the DSC curve of HP-β-CD and the specific peaks of DSC curve of CUR disappeared. The obtained DSC results confirm the formation of the inclusion complex from CUR and HP-β-CD (29).

## 2.2. Anti-oxidant and anti-inflammatory activity assessment of free CUR and CUR-HP-β-CD inclusion complex

The anti-inflammatory activities of CUR and CUR/HP-β-CD inclusion complexes were comparatively evaluated by analyzing of lipoxygenase (LOX) enzyme inhibition. As seen in Table 1, % LOX inhibitions of free CUR and CUR/HP-β-CD inclusion complex were found as 8.7±2.0% and 25.3±2.7% respectively. The anti-inflammatory activity of the CUR/HP-β-CD complex was found significantly higher than free CUR according to the LOX inhibition assay results ( $p < 0.0001$ ).

**Table 1.** Anti-oxidant and anti-inflammatory activities of free CUR and CUR-HP-β-CD inclusion complex (values followed by ± are SD of the mean, n = 3).

Formulation	ABTS assay (% radical scavenging activity, at 7.5 µg/mL CUR equivalent solution)	LOX assay (% inhibition, at 25 µg/mL CUR equivalent solution)
Free CUR	85.0 ± 1.2	8.7 ± 2.0
CUR:HP-β-CD inclusion complex	97.1 ± 0.7	25.3 ± 2.7

The total antioxidant capacity of CUR/HP-β-CD inclusion complex was analyzed by ABTS•+ scavenging methods. As shown in Table 1, While ABTS radical scavenging rate of free CUR was 85.0 ± 1.2%, this capacity increased to 97.1 ± 0.7% with CUR/HP-β-CD inclusion complex. ABTS radical scavenging activity with CUR/HP-β-CD Inclusion complex was significantly higher compared to free curcumin ( $p = 0.007$ ). Our results indicated that HP-β-CD inclusion complex of CUR could effectively scavenge the ABTS free radical. These results were interpreted as it is possible to provide increased antioxidant activity

with the CUR/HP-β-CD inclusion complex, which can be used in innovative formulation approaches and dosage form designs (25).

### 2.3. Characterization of *in situ* gel formulations

#### 2.3.1. Gelation temperature and clarity

In terms of ease of application, *in situ* gels should have a low viscosity at room temperature. Additionally, a sol-gel transition should occur at body temperature (35-36 °C) upon application to the eye, resulting in the formation of a transparent structure. One of the most important factors in improving patients' compliance of *in situ* gels is clarity (20). In this study, the optimum *in situ* gel formulation containing CUR was selected among formulations containing various ratios of PF127 and CH. Examining the *in situ* gel formulations prepared with various polymer ratios revealed that all formulations were clear with the exception of the FB9 formulation, which had a high concentration of 25% PF127 and 3% CH. Other formulations provided adequate transparency (Table 2). Another important factor for ocular applications is the gelling temperature. As the low viscosity of the formulation at room temperature increases after application to the eye, the contact time between the formulation and the ocular surface can be increased (30). Analysis of all formulations in terms of gelling temperature showed that the gelation temperature ranged from 16 °C to 35°C (Table 2). The main reason for this situation was considered to be the polymer concentration. The increase in PF127 and CH concentration results in a decrease in gelation temperature. In this context, it was determined that the FB1 formulation started to gel around 35°C. Our findings and comments were considered to be compatible with the literature (31). At temperatures below the critical micelle temperature (CMT), at which the critical micelle concentration (CMC) occurs, PF127 keeps all molecules in an aqueous medium apart. The hydrophilic chains of PF127 start to form micelles around the hydrophobic core as the temperature rises over the CMT. In other words, the CMT value falls as the PF127 concentration rises. The gelling temperature is significantly impacted by CMT. The pluronic concentration is the primary factor at the gelling temperature. In water, they create lattice-like structures as the concentration rises, lowering the gelation temperature (22). Within the scope of the study, the amount of pluronic polymer was reduced in order to enable gelation to occur at corneal temperature. When the literature is examined, it is seen that the findings are consistent (31).

**Table 2.** *In vitro* characterization analysis results of *in situ* gels

Formulation	pH (±SD)	Gelation temperature (°C±SD)	Viscosity (centipoise) 25°C	Viscosity (centipoise) 35°C	Clarity
FB1	5.98±0.01	35±0.3	294±17	10052±111	Clear
FB2	5.95±0.02	32±0.4	342±29	14578±172	Clear
FB3	5.91±0.03	30±0.4	401±26	17845±227	Clear
FB4	5.89±0.06	29±0.5	665±32	24842±442	Clear
FB5	5.90±0.03	27±0.1	1067±45	35642±363	Clear
FB6	5.92±0.04	25±0.2	8782±103	39512±544	Clear
FB7	5.88±0.03	18±0.2	21085±577	57142±994	Clear
FB8	5.86±0.04	17±0.3	29085±428	65847±942	Clear

FB9	5.84±0.105	16±0.2	35855±647	69264±879	Not Clear
-----	------------	--------	-----------	-----------	-----------

### 2.3.2. pH value

Since the eye structure has a sensitive surface, pH changes have a significant effect on the eye. The pH of the formulation applied to the ocular surface should be between 5.0 and 7.4. Applications outside of this range may cause eye discomfort, increase tear production as a physiological reflex to adjust pH, and this may have a negative effect on ocular bioavailability. When evaluated in this context, literature data show that CUR is stable at pH 6, which is considered suitable for the formulations (32, 33). The pH of every *in situ* gel formulation has been discovered to be around 5.85. It has been interpreted that all formulations will not have an irritant effect when applied to the eye in terms of pH value.

### 2.3.3. Viscosity

While the viscosity of the formulation containing 25% PF127 and 3% CH at 25°C was 35855±647 cp, the viscosity of the formulation containing 15% PF127 and 1% CH was 294±17 cp (Table 2). This example demonstrates the significant impact that polymer concentration has on viscosity. Examining the literature revealed that the findings were consistent (30). Rheological characteristics are a crucial factor in increasing the effectiveness and patient compliance of *in situ* gel formulations. While high viscosity *in situ* gels can cause various problems when applied, low viscosity *in situ* gels are quickly removed from the eye surface with tears. The high viscosity of an ocular formulation is undesirable as it often tends to leave a noticeable residue on the lateral aspect of the eyelid following application. Therefore, providing the appropriate viscosity to the ocular region is an important formulation parameter. By using *in situ* gel formulations with pseudoplastic behavior, it is possible to reduce the undesirable effects of ocular reflexes such as blinking on the formulation. Pseudoplastic flow of formulation provides comfortable application and increases corneal contact time (34). The impact of angular velocity changes on viscosity is depicted in Figure 7. All *in situ* gel formulations at respective gelling temperatures showed pseudoplastic flow (shear thinning system) similar to tear fluid when the rheological characteristics were studied.

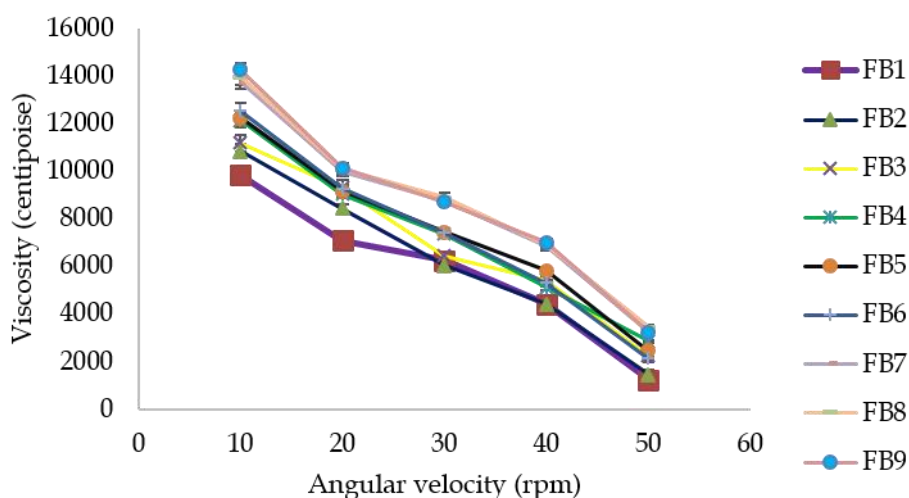


**Figure 7.** Rheological behaviors of *in situ* gelling formulations.

When the literature is examined, it has been determined that the ideal viscosity for ocular formulations is between 50 and 150,000 cp (30). Formulations were evaluated in this context and viscosity values were measured at 10 rpm at both 25 °C and 35 °C for the NSL and NFS formulations. As a result of the analysis, it was determined that both formulations were in the appropriate viscosity range.

After characterization studies (pH value, gelling temperature, clarity and viscosity) for all *in situ* gel formulations, the optimum formulation was determined. For the selected formulation, CUR (0.5% w/v) or CUR:HP-β-CD (0.5% w/v) was included and coded as NFS and NSL, and formulation contents are presented in Table 3. NFS and NSL were observed to appear clear, have a pH of about 5.9, and gel at 35°C and 34°C, respectively. To evaluate their viscosity and the effect of temperature, they were examined at 15°C, 20°C, 25°C, 30°C and 35 °C for both formulations (Figure 8). It was found that the viscosities of both

formulations increased as the temperature increased. When the literature was examined, it was observed that the viscosity increased with increasing temperature and the compatibility of the results was determined (35).

**Table 3.** Physical properties of drug containing formulations and their component.

Formulation components and physical properties	NFS	NSL
CUR (% w/v)	0.5	0
CUR:HP-β-CD (% w/v)	0	0.5
PF-127	15	15
Chitosan	1	1
BC	0.001	0.001
EDTA	0.05	0.05
Sodium chloride	0.2	0.2
Distilled Water	100 ml	100 ml
pH (±SD)	5.98±0.01	5.89±0.02
Gelation temperature (°C±SD)	35±0.3	34±0,2
Viscosity (centipoise) 25 °C	294±15	300±29
Viscosity (centipoise) 35 °C	10052±452	10202±422
Clarity	Clear	Clear

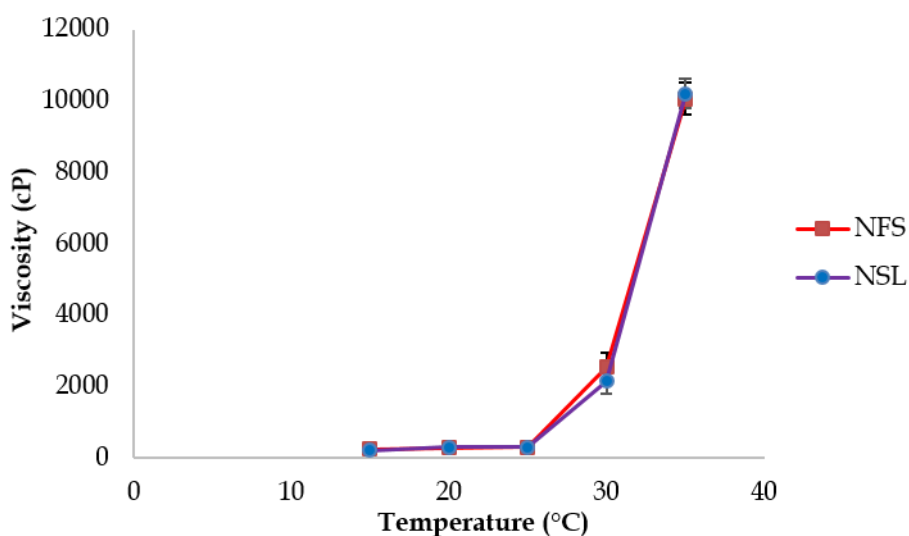


**Figure 8.** Viscosity profiles of in situ gels at different temperatures.

#### 2.3.4. Drug loading

As a result of the evaluation of the drug loading efficiency of the prepared gel formulations, over 95% CUR recovery was detected for the NFS and NSL gel systems (Figure 9).

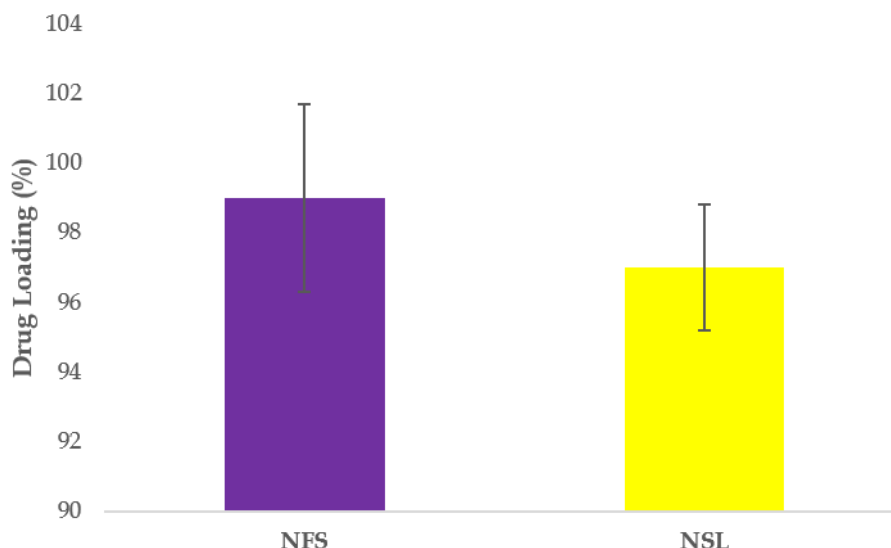


**Figure 9.** Drug loading given in percentages for CUR (n=3)

### 2.3.5. Drug release

CUR (0.5% w/v) or CUR:HP-β-CD (0.5% w/v equivalent CUR) loaded formulations, NFS and NSL, were used for the *in situ* gel drug release experiments, which were carried out at 35°C in release medium (isotonic phosphate buffer at pH 7.4: ethanol, 1:1). *In vitro* release profiles of CUR from formulations are presented in Figure 10. NFS exhibited >63% drug release after two hours, and at the end of 3 hours, 77% of the CUR was released. NSL exhibited >75% drug release after two hours due to CD complex in the formulation. NSL released all the drug at the end of the sixth hour. It is hypothesized that the two formulations' various solubilities are what caused this variation in release. Compared to CUR, CUR:HP-β-CD complex has a higher water solubility and a quicker release. When the literature was examined, it became clear that the solubility correlated with the rate at which the active ingredient was released. Levofloxacin and metronidazole were placed on *in situ* gels in one study, but further *in vitro* release assays revealed that Levofloxacin HCL released more quickly due to its higher solubility [39]. Another study by Polat et al. investigated the release characteristics of besifloxacin HCl and besifloxacin HCl/CD complex, finding that the complex's improved solubility resulted in a release time reduction from seven days to three days (19).

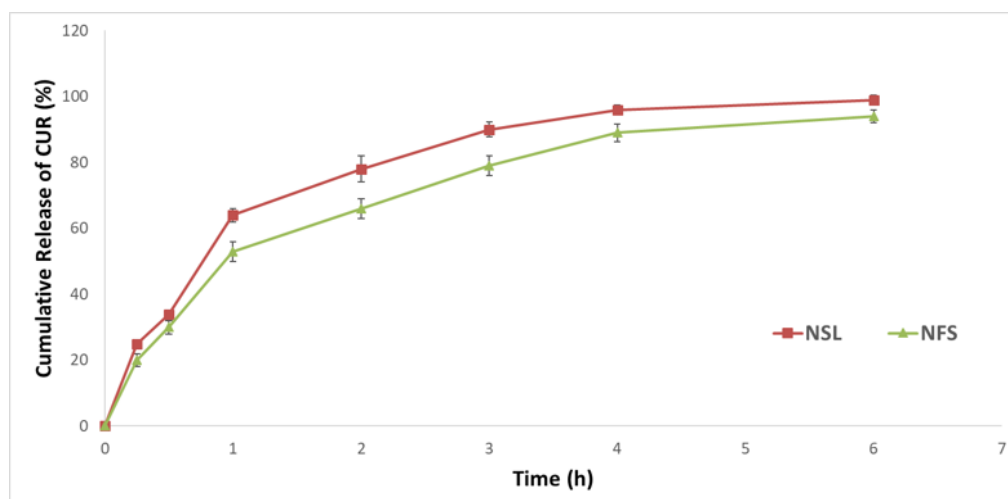


**Figure 10.** Cumulative release of CUR from *in situ* gel formulations

## 2.4. Release kinetic study

*In vitro* release profiles of CUR from *in situ* gel formulations were investigated in various kinetic models. Mathematical modeling has been carried out in order to elucidate the release mechanisms, which

have a valuable view in the characterization of new drug delivery systems. In this context, 8 kinetic models (Zero order, first order, Higuchi, Korsmeyer-Peppas, Peppas-Sahlin, Hopfenberg, Weibull and Baker-Lonsdale) and 4 significant parameters ( $R^2$ ,  $R^2_{\text{adjusted}}$ , AIC and MSC) for the detailed evaluation of the active substance released from *in situ* gel formulations and to elucidate the release mechanisms were analyzed (36). For this purpose, critical parameters were calculated in each formulation within the scope of kinetic modeling analysis studies and a comprehensive evaluation was carried out. The critical parameters of the release kinetic modeling studies are presented in the Table 4., and the graphical reports from the DDSolver program are presented in the Figure 11. As can be seen in Figure 11., the models that are considered to be the most compatible in terms of mathematical analysis can be confirmed graphically with the compatibility of predicted and observed values.

Model and equation / Formulation		Evaluation criteria						
		Parameter	$R^2$	$R^2_{\text{adjusted}}$	AIC	MSC	$n/m^*$	
<b>Zero-order</b> $F=k_0*t$	NSL	k0	0.375	0.4199	0.4199	70.9615	-0.1938	-
	NFS	k0	0.342	0.5768	0.5768	67.2583	0.1758	-
<b>First-order</b> $F=100*[1-\text{Exp}(-k_1*t)]$	NSL	k1	0.013	0.9839	0.9839	42.2805	3.3913	-
	NFS	k1	0.008	0.9619	0.9619	48.0064	2.5822	-
<b>Higuchi</b> $F=k_H*t^{0.5}$	NSL	kH	6.175	0.9214	0.9214	54.9717	1.8049	-
	NFS	kH	5.570	0.9652	0.9652	47.2695	2.6744	-
<b>Korsmeyer-Peppas</b> $F=k_{KP}*t^n$	NSL	kKP	10.870	0.9511	0.9429	53.1790	2.0290	0.401
	NFS	kKP	5.705	0.9632	0.9571	49.7111	2.3692	0.500
<b>Peppas-Sahlin</b> $F=k_1*t^m+k_2*t^{(2*m)}$	NSL	k1	10.571	0.9708	0.9591	51.0466	2.2956	0.450
	NFS	k1	8.253	0.9807	0.9730	46.5571	2.7634	0.450
<b>Hopfenberg</b> $F=100*[1-(1-k_{HB}*t)^n]$	NSL	kHB	0.003	0.9736	0.9692	48.2416	2.6462	4.125
	NFS	kHB	0.002	0.9618	0.9554	50.0238	2.3301	4.500
<b>Weibull</b> $F=100*\{1-\text{Exp}[-((t-T_i)^\beta)/\alpha]\}$	NSL	$\beta$	0.775	0.9920	0.9887	40.7289	3.5853	-
	NFS	$\beta$	0.705	0.9948	0.9927	36.1252	4.0674	-
<b>Baker-Lonsdale</b> $3/2*[1-(1-F/100)^{2/3}]-F/100=k_{BL}*t$	NSL	kBL	0.001	0.9792	0.9792	44.3325	3.1348	-
	NFS	kBL	0.001	0.9827	0.9827	41.6837	3.3726	-

**Table 4.** In all models, F is the fraction (%) of drug released in time t, k<sub>0</sub>: zero-order release constant, k<sub>1</sub>: first-order release constant, k<sub>H</sub>: Higuchi release constant, k<sub>KP</sub>: release constant incorporating structural and geometric characteristics of the drug-dosage form, k<sub>HB</sub>: Hopfenberg release constant, n: is the diffusional exponent indicating the drug-release mechanism, m: diffusional exponent and similar exponent like "n", m use in Peppas-Sahlin model equation only,  $\alpha$ : is the scale parameter which defines the time scale of the process;  $\beta$ : the shape parameter which characterizes the curve as either exponential ( $\beta=1$ ; case 1), sigmoid, S-shaped, with upward curvature followed by a turning point ( $\beta > 1$ ; case 2), or parabolic, with a higher initial slope and after that

consistent with the exponential ( $\beta < 1$ ; case 3),  $T_i$ : the location parameter which represents the lag time before the onset of the dissolution or release process and in most cases will be near zero (39). Values shown in *italics and bold* in the table are selections made according to criteria.

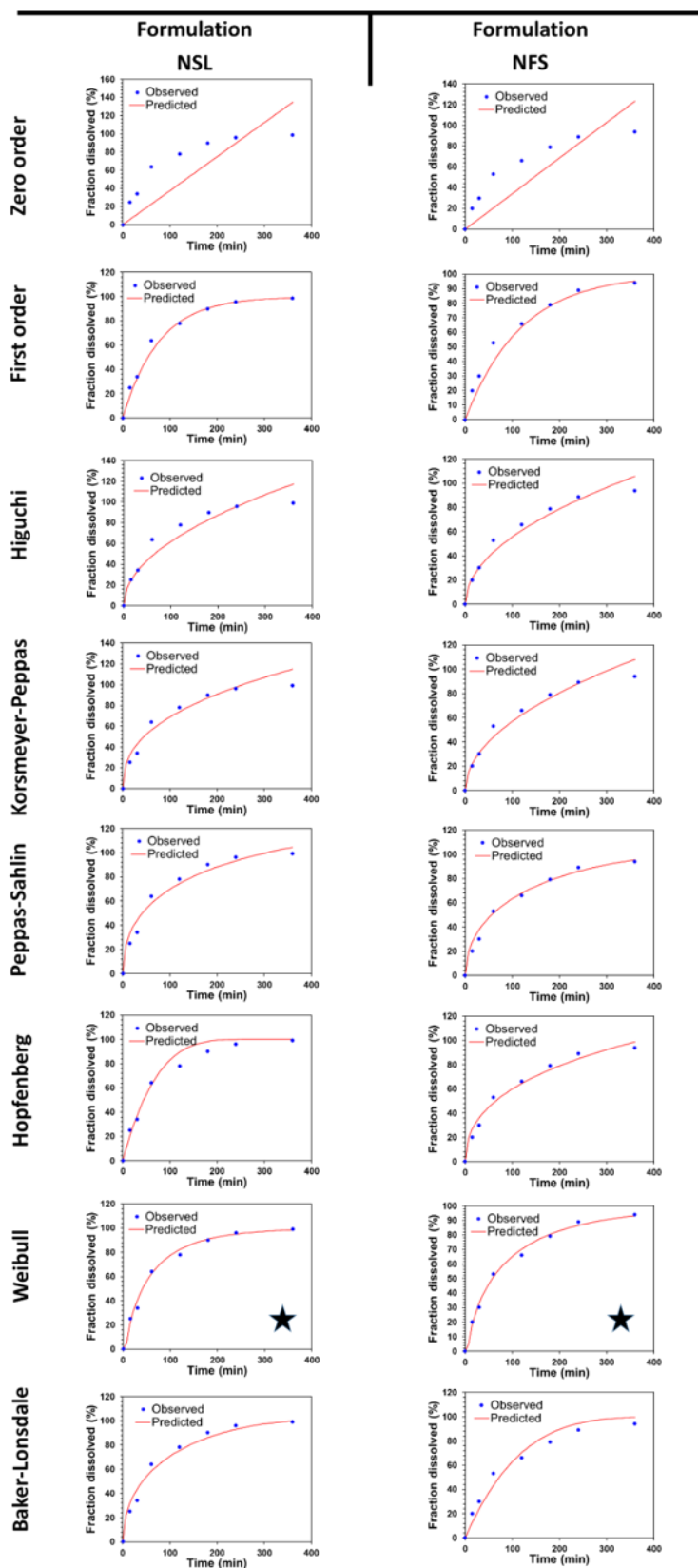


**Figure 11.** Results of release kinetics modeling analyses graphs of CUR release from *in situ* gel formulations

In addition, *In vitro* release profiles from formulations were analyzed by calculating  $f_1$  and  $f_2$  values in terms of similarities and differences. It was evaluated that the release profiles of both formulations were similar with  $f_1$  value less than 15 and  $f_2$  value greater than 50. Although a faster release profile was observed with CD complexation, it was determined that both formulations have similar release profiles in terms of model-independent evaluation. This situation was interpreted as the gel formulation being the major effective factor in the release profiles for the formulations prepared in this study. The fact that the gel formulations were the same in both formulations was interpreted as resulting in the release profiles being essentially similar (Table 5).

**Table 5.** Evaluation of the differences and similarities of the release profiles of the formulations with the difference ( $f_1$ ) and similarity ( $f_2$ ) factors

<i>In situ</i> Gel Formulation	NFS	
	Difference Factor ( $f_1$ )	Similarity Factor ( $f_2$ )
NSL	11.32	54.91

$R^2$  and  $R^2_{\text{adjusted}}$  values for zero order, first order, Higuchi, Korsmeyer-Peppas, Peppas-Sahlin, Hopfenberg and Baker-Lonsdale models were calculated to be smaller than the Weibull model for both formulations. Furthermore, the AIC value has been utilized as a metric to identify the best fitting model and to clarify the kinetic mechanism at an advanced stage. On the other hand, MSC has attracted attention as a model selection criterion and has seen an increase in release kinetics modeling applications recently. The lowest AIC value and the highest MSC value were also observed in the weibull model. From this point, there is a clear fit with higher correlation in the Weibull model compared to other models. In the light of all this information, when all parameters are evaluated together (for the highest  $R^2$ ,  $R^2_{\text{adjusted}}$ , MSC and lowest for AIC), Weibull model are clearly considered more compatible than other models. According to the Weibull model (a mechanism in which the amount of drug release is a function of time), the shape parameter " $\beta$ " is a critical value and is meaningful in elucidating the mechanism of release kinetics (37). " $\beta$ "  $\leq 0.75$  represents Fickian diffusion, while  $0.75 < \beta < 1$  expressed Fickian diffusion and swelling controlled release. Within the scope of the Weibull model, " $\beta$ " values were calculated as 0.775 and 0.705 for CUR for NSL and NFS formulations, respectively. From this point of view, it has been interpreted that the release of free CUR from *in situ* gel formulations occurs predominantly according to the Fickian/diffusion-controlled mechanism, while in the form of cyclodextrin complex, it occurs under the control of Fickian diffusion and swelling controlled by a combined mechanism. In the formulations prepared within the scope of the study, Fickian diffusion (pure diffusion phenomenon) and non-Fickian release mechanisms (due to the relaxation/swelling of the polymer chains between the networks) can be occurred together. In addition, it has been observed that the release kinetic mechanism may change with approaches such as formulation approach and CD complex formation, even if the same active ingredient is present in the *in situ* gel formulation. From this point of view, it is evaluated that solvent diffusion rate and polymeric chain relaxation are effective on the *in vitro* release mechanism. In the literature, there are release profiles from poloxamer-structured *in situ* gel systems that fit multiple/different kinetic mechanisms. This situation may also be related to experimental conditions, polymer ratio, physicochemical properties of the drug/active substance used. These results might be explained by the burst release that occurred during the early phase of *in vitro* release, which was mostly due to drug diffusion through the polymeric framework and Fickian diffusion occurring close to the gel surface. Due of the deterioration of the polymeric framework, poloxamer chain relaxation may be linked to later stage release. In other words, the findings indicated that the diffusion and erosion of the gel forming material are the mainly factors controlling the release of drug/active ingredients from *in situ* gel formulation (38).

### 3. CONCLUSION

In this study, inclusion complexes of CUR:HP- $\beta$ -CD were prepared with freeze drying methods. As a result of the comprehensive characterization studies carried out for the prepared complexes, it was determined that the CUR and HP- $\beta$ -CD complexation was carried out successfully. *In situ* gel formulations were prepared to design a dosage form containing CUR:HP- $\beta$ -CD inclusion complexes for application in ocular diseases. For this purpose, *in situ* gel systems containing different ratios of PF127 and CH were prepared and evaluated. The pH, clarity, gelation temperatures, and rheological behavior of each formulation were evaluated. All formulations displayed pseudoplastic flow similar to tears, as evidenced by their rheological characteristics. The gelation temperature and viscosity of the FB1 formulation were determined as  $35 \pm 0.3^\circ\text{C}$  and  $294 \pm 17$  poise, respectively, and concluded that it was suitable for the ocular application. Subsequently, the optimized formulation was loaded with CUR and CUR:HP- $\beta$ -CD. In this formulation, the pH was 5.98, the gelation temperature was around  $35^\circ\text{C}$ , and it demonstrated pseudoplastic behavior. Moreover, prepared formulation exhibited up to 6 hours of CUR release. The CUR from *in situ* gel formulation would be released over a longer period of time than with traditional eye drops thanks to *in situ* gel's prolonged residence duration on the eye. According to the comprehensive release kinetics study, CUR release from the *in situ* gel formulation was found to be compatible with the Weibull model with high correlation. When all the results within the scope of the study are evaluated together; CUR:HP- $\beta$ -CD inclusion complexes have been successfully prepared and extensively characterized. In addition, it was designed as an *in situ* gel formulation that can be used in ocular diseases as an advanced step and *in vitro* characterization of the formulations was completed. In order to increase the power of the study, a comprehensive release kinetic study was also carried out. As a result; An innovative formulation approach, with detailed *in vitro* characterization studies, has been proposed for use in ocular diseases. It is also considered that the results of this study will inspire future studies.

## 4. MATERIALS AND METHODS

### 4.1. Materials

Curcumin ( $\geq 94\%$  (curcuminoid content), powder), (2-Hydroxypropyl)- $\beta$ -cyclodextrin, Pluronic® F-127 (Poloxamer), Benzalkonium chloride, EDTA (Ethylenediaminetetraacetic acid), dialysis cellulose tubing membrane (average flat width 25 mm, MWCO: 14,000 Da), ABTS (2,2'-Azino-bis (3-ethylbenzothiazoline-6-sulfonic acid) diammonium salt) and Lipoxidase from Glycine max (soybean) were purchased from Sigma&Aldrich. Chitosan (Protasan UP G-113; Mw: <200 kDa) was purchased from Novamatrix, Norway. All other chemicals used were of analytical grade and obtained from Sigma&Aldrich.

### 4.2. The quantification of CUR in inclusion complex by UV-VIS spectrophotometry

Quantification of CUR in inclusion complexes was analyzed spectrophotometrically (Shimadzu UV 1800, USA). Standard solutions of pure CUR were prepared in ethanol concentration ranges 0.5-6.0  $\mu\text{g}/\text{mL}$ . The absorbance of standard solution was measured at 424 nm and the calibration curve was determined. The spectrophotometric method's validation was carried out in accordance with ICH guidelines (40). Linearity, accuracy, precision, repeatability, limit of detection (LOD), and limit of quantification (LOQ) were assessed within the context of the validation of the spectrophotometric technique utilized for CUR quantification. The correlation coefficient of calibration curve was calculated ( $r^2=0.9995$ ). LOD and LOQ, as the expression of sensitivity of the method, was determined as 0.0165  $\mu\text{g}/\text{mL}$  and 0.0539  $\mu\text{g}/\text{mL}$ , respectively. To calculate the complexation efficiency, 10 mg of the prepared CUR-HP- $\beta$ -CD inclusion complex was weighed and dissolved in 10 ml of ethanol to determine the CUR content of the complex. The blank ethanol solution was used as a reference for baseline.

The complexation efficiency (CE) was calculated according to Li et al. (41). CE (%) was described as the ratio between the amount of CUR in the inclusion complex and the total amount of CUR added initially. CE was calculated by the following equation (1):

$$\text{CE} = \frac{CCc}{CTc} \times 100$$

(1) where CCc is mass of complexed CUR and CTc is mass of total weight of CUR added initially.

### 4.3. Preparation of CUR-HP- $\beta$ -CD complex

A modified cosolvency-lyophilization method was applied for the preparation of CUR:HP- $\beta$ -CD inclusion complexes (41). Briefly, a solution of CUR in ethanol is slowly dropped into the aqueous solution

of CD, at a molar ratio of 1:3 (CUR:HP-β-CD). The prepared suspension was mixed on a magnetic stirrer at 400 rpm for 48 hours at 35°C. Excess amount of HP-β-CD is used in order to increase the complexation yield. After 48 hours, the mixture was filtered through 0.22 μm filter and then lyophilized (48 hours) in order to get light yellow fully powder. The lyophilisation procedure was as follows: pre-freezing at -80°C for 3 h, freeze-drying at pressure <10 Pa for 48 h. The whole experimental process was mostly performed in the dark. CUR complexation efficiency (EE) was calculated according to the equation in Section 4.2.

#### 4.4. Characterization of CD inclusion complex

##### 4.4.1. Phase-solubility studies

The phase-solubility study was carried out by the method reported by Higuchi and Connors (42). In this context, it was studied with the principle of examining the correlation between HP-β-CD concentration and the amount of dissolved CUR (21). Briefly, HP-β-CD aqueous solution was prepared at increasing concentrations (0-10 mM) and an excess and constant amount of CUR was added to these solutions. The resulting mixture was stirred at room temperature for seven days with a magnetic stirrer in the dark. At the end of the seventh day, all mixtures containing HP-β-CD and CUR were filtered using 0.45 μm cellulose membrane filters. The amount of CUR in the supernatant was analyzed by UV spectrophotometer. At the end of the study, the phase-solubility diagram was drawn by presenting the correlation between the amount of dissolved CUR and the HP-β-CD concentration. Phase-solubility diagrams can be classified in various types (43). Within the scope of this classification, the diagrams are listed as follows; AP, AL, AN, BS and BI. Complexation stability constant (CST) and complex efficacy (CE) are calculated by the equation reported by Loftson et al (19, 43). The CST is calculated according to equation (2);

$$CST = \frac{Slope}{S_0(1-Slope)} \quad (2)$$

The phase-solubility diagram is analyzed with the slope of the linear regression as slope and the intrinsic CUR solubility as  $S_0$ , which is  $1.65 \times 10^{-5}$  mM. The CE was calculated according to equation (3) (29, 43);

$$CE = \frac{Slope}{1-Slope} \quad (3)$$

##### 4.4.2. Characterization of inclusion complex

In order to conduct a comprehensive *in vitro* characterization study of CUR:HP-β-CD inclusion complexes; Scanning electron microscopy (SEM), Fourier transform-infrared spectrometer (FT-IR) and X-ray diffraction (XRD), Differential scanning calorimetry (DSC) analyzes were performed.

Scanning Electron Microscope (SEM) (LEO 440) was used to visualize surface morphology of the pure components and CUR:HP-β-CD inclusion complex.

Fourier transform-infrared spectrometer (Perkin Elmer 400 FT-IR spectrometer) was utilized to characterize functional groups of pure CUR, HP-β-CD polymer, CUR:HP-β-CD inclusion complex and CUR/HP-β-CD physical mixture. A Raman spectrophotometer (WITec alpha 300 M + micro-Raman system with 532 nm laser source) was used for the Raman analysis of CUR: HP-β-CD inclusion complex.

The X-ray diffraction (XRD) spectrums of pure components and inclusion complex were ensured using an advanced XRD diffractometer (Bruker AXS D8). the samples were investigated in the  $2\theta$  range of  $2^\circ$ - $70^\circ$ .

Differential scanning calorimetry (DSC) analysis performed with a Exstar 7000 (Su Nanotechnology). DSC curves of the pure component and the inclusion complex, obtained by heating from  $20^\circ$  C to  $300^\circ$  C under a nitrogen flow of 50 ml/min.

#### 4.5. Anti-oxidant and anti-inflammatory activity assessment

##### 4.5.1. Lipoxygenase (LOX) assay

Lipoxygenase assay was performed in 96-well microplates according to the modified method developed by Wasldige and Hayes (44) (45). An aliquot of 50 μL of LOX (Sigma, L6632) in 50mM Tris HCl buffer, pH7.4 (final concentration, 100ng protein/mL), and 20 μL of sample were incubated at  $25^\circ$  C for 5

minutes. As a control, 20 μL of buffer containing 50 μL of LOX solution and 0.2% v/v DMSO (final concentration) was used. The reaction was started by adding 50μL of linoleic acid (final concentration, 140°M) in 50mM Tris HCl buffer, pH 7.4. The reaction mixture was incubated at 25°C for 20 minutes in the dark. The experiment was terminated by adding 100 μL of freshly prepared FOX reagent (sulfuric acid (30 mM), xylenol orange (100μM), iron (II) sulfate (100 μM), methanol/water (9:1)). It was then treated with Fe<sup>3+</sup>-dye complex for 30 minutes at 25°C. Absorbances were measured at 560 nm in a microplate reader (BiotEKM Synergy HT, USA) (45). The % enzyme inhibitions of the samples were calculated using the following equation (4);

$$\text{Inhibition \%} = \frac{(\text{Abscontrol} - \text{Abssample})}{\text{Abscontrol}} \times 100 \quad (4)$$

#### 4.5.2. ABTS assay

ABTS radical scavenging effect, which is one of the antioxidant activity determination methods, was made by using 96-well microplates, by modifying the method developed by Re et al (46). A solution of green ABTS•+ radical was generated by keeping K<sub>2</sub>S<sub>2</sub>O<sub>8</sub> (2.45 mM, final concentration) with (7 mM) ABTS aqueous solution in the dark for 12-16 hours. The solution was adjusted to have an absorbance of 0.700 (± 0.2) at 734 nm by dilution with ethanol. For each sample, 20 μl of the ethanolic test solution (at a final concentration of 7.5 μg/mL CUR equivalent solution) and 180 μl of ABTS radical solution were mixed in microplates and then incubated for 6 minutes. At the end of the period, the absorbances of the mixtures were read at 734 nm in the microplate reader. All samples were studied in three parallels and mean values were recorded. The radical scavenging activities % of the samples were calculated using the following equation (5).

$$\text{Radical scavenging activity \%} = \frac{(\text{Abscontrol} - \text{Abssample})}{\text{Abscontrol}} \times 100 \quad (5)$$

#### 4.6. Preparation of *in situ* gel formulation

A modified cold technique was used to prepare the *in situ* gel formulations (47). All Pluronic F-127 (PF127) solutions (15, 20% and 25% w/v) used in this study were prepared by mixing the polymer with cold water (4°C). Briefly, polymer solutions were cooled for 24 hours. Then, CH (1% w/v) solution was prepared. For this purpose, CH was first dissolved in acetic acid solution (2% v/v) and then cooled for 24 hours. At the same temperature, the CH solution was then added to the PF-127 solution. Each sample was stored at 4 °C before use. The compositions of the *in situ* gel formulations are presented in Table 6.

**Table 6.** Components of *in situ* gel formulation (BC; benzalkonium chloride, EDTA; Ethylenediaminetetraacetic acid, PF127; Pluronic F-127)

Formulation	Composition of the each formulation (% , w/w)					
	PF127	Chitosan	BC	EDTA	Sodium chloride	Distile water (qs)
FB1	15	1	0,001	0,05	0,2	100
FB2	15	2	0,001	0,05	0,2	100
FB3	15	3	0,001	0,05	0,2	100
FB4	20	1	0,001	0,05	0,2	100
FB5	20	2	0,001	0,05	0,2	100
FB6	20	3	0,001	0,05	0,2	100
FB7	25	1	0,001	0,05	0,2	100
FB8	25	2	0,001	0,05	0,2	100
FB9	25	3	0,001	0,05	0,2	100

#### 4.7. Characterization of *in situ* gel formulations

Gelation temperature, pH, clarity and viscosity were analyzed for all formulations containing various concentrations of PF127 and CH (FB1–FB9). Characterization studies were performed for all formulations presented in Table 2.

#### 4.7.1. pH

pH measurements of the prepared formulations were carried out using a pH meter (Hanna, Germany). All analyzes were performed in triplicate (n=3).

#### 4.7.2. Clarity

After gelation, the clarity of the *in situ* gel formulation was evaluated for all formulations by examining them in bright light against a dark background (48).

#### 4.7.3. Viscosity

The rheological properties of all formulations were first evaluated by measuring viscosity at both 25°C and 35°C using a rotational viscometer (Fungilab, USA) with an R5 spindle rotating at 10 rpm. All analyzes were performed in triplicate (n=3).

#### 4.7.4. Rheological evaluation of formulations

The rheological behavior of the *in situ* gel formulations were assessed using viscometer (Fungilab, USA) with R5 spindle. The spindle rotates at 1, 2.5, 5, 10, 20, and 50 rpm. At the temperature when gelation occurs, the viscosities of *in situ* gels were measured. At various angular velocities, viscosities were computed and flow curves were calculated. All analyzes were performed in triplicate (n=3).

### 4.8. Preparation of CUR: HP-β-CD containing *in situ* gel formulation

Formulations containing CUR:HP-β-CD inclusion complex were prepared by using the *in situ* gel formulation determined after the evaluation of pH, viscosity, clarity, rheological properties and gelling temperature. The chosen formulations were supplemented with precise amount of CUR (0.5 % w/v) or CUR:HP-β-CD (0.5% w/v equivalent to CUR). These formulations are coded, in order, as follows: NFS and NSL. The components of NFS and NSL formulations and their characterization data are presented in Table 3.

### 4.9. Drug content

After the formulations were prepared, the CUR contents of the *in situ* gel formulations were calculated using the UV-vis spectrophotometric quantification method described in the section 4.2. For this purpose, 1 mL gel formulation was diluted in 2 mL ethanol and then sonicated in a water bath for 1 hour, and measurements were made according to the equation (6).

$$\text{Drug Loading of in situ gel formulations (\%)} = \frac{\text{Amount of CUR analyzed}}{\text{Initial total weight of CUR}} \times 100 \quad (6)$$

### 4.10. *In vitro* release studies

*In vitro* release experiments can be performed with the dialysis membrane method for *in situ* gel formulations (49). In this context, the formulation containing CUR (100uL) was transferred to the dialysis bag, then securely bound and immersed in 5 mL pH 7.4 isotonic phosphate buffer at 37 °C, *in vitro* release studies were carried out under sink conditions. At different time points (15, 30, 60, 120, 180, 240 and 360 min) the medium was removed and replaced with fresh buffer. Then, at the end of the experiment, the *in vitro* release profile was determined by calculating the cumulative amount of CUR released at each time point. All experiments conducted triplicate(n=3).

### 4.11. Release kinetics study

*In vitro* release profiles of CUR from *in situ* gel formulations were analyzed with DDSolver software. By using DDSolver software, computation time is reduced, and computational errors can be eliminated. In this context, several mathematical models were applied to investigate active ingredient release kinetics from formulations (Zero order, First order, Higuchi, Korsmeyer-Peppas, Peppas-Sahlin, Hopfenberg, Weibull and Baker-Lonsdale). After analyzing the *in vitro* drug release profiles from *in situ* gel formulations, data were computed with DDSolver software to determine the meaningful and important four criteria for the selection of the "best fit" models; coefficient of determination (R<sup>2</sup>), adjusted coefficient of determination (R<sup>2</sup><sub>adjusted</sub>), Akaike Information Criterion (AIC) and Model Selection Criterion (MSC). The highest R<sup>2</sup>, R<sup>2</sup><sub>adjusted</sub> and MSC values and the lowest AIC values were used to determine the model with higher correlation and higher goodness of fit to *in vitro* release data (39, 50). Furthermore, drug release profiles from *in situ* gel

formulations were evaluated in terms of similarities and differences with model-independent approach according to the “difference (f1)” and “similarity (f2)” factors (39, 51). To evaluate release profiles of formulations, the difference factor (f1) and similarity factor (f2) were computed using a method outlined in the Guidance for Industry from the FDA's Center for Drug Evaluation and Research (CDER) (52). Following equations were used for the mathematical calculation of f1 and f2 factors (53). It is noted that the two release profiles appear to be similar based on f1 values between 0 and 15 and f2 values between 50 and 100 (54).

$$f1 = \{(\sum_{t=1}^n |R - T|) / (\sum_{t=1}^n R)\} \times 100 \quad (7)$$

$$f2 = 50 \cdot \log \left[ \frac{100}{1 + \frac{\sum_{t=1}^n |Rt - Tt|^2}{n}} \right] \quad (8)$$

#### 4.12. Statistical analysis

All experiments were performed in triplicate and results are given as mean ± standard deviation. One-way ANOVA analysis was applied for multiple group comparisons. Tukey's pairwise and Dunnett tests were used to evaluate the significant differences between the means at the p<0.05 level.

**Acknowledgements:** *In vitro* characterization analyzes of the complexes were performed at Erciyes University ERNAM and TAUM research centers.

**Author contributions:** Concept – S.Ü., H.K.P.; Design – S.Ü., D.Y., H.K.P.; Supervision – S.Ü.; Resources – S.Ü., D.Y., H.K.P., E.K.Ş.; Materials – S.Ü.; Data Collection and/or Processing – S.Ü., D.Y., H.K.P., E.K.Ş.; Analysis and/or Interpretation – S.Ü., D.Y., H.K.P., E.K.Ş.; Literature Search – S.Ü., D.Y.; Writing – S.Ü., D.Y., H.K.P., E.K.Ş.; Critical Reviews – S.Ü., D.Y., H.K.P., E.K.Ş.

**Conflict of interest statement:** The authors declared no conflict of interest.

#### REFERENCES

- [1] Guo C, Cui F, Li M, Li F, Wu X. Enhanced corneal permeation of coumarin-6 using nanoliposomes containing dipotassium glycyrrhizinate: *in vitro* mechanism and *in vivo* permeation evaluation. *RSC Advances*. 2015;5(92):75636-47. [CrossRef]
- [2] Bucolo C, Drago F, Salomone S. Ocular drug delivery: a clue from nanotechnology. *Frontiers Media SA*; 2012. p. 188. [CrossRef]
- [3] Joseph RR, Venkatraman SS. Drug delivery to the eye: what benefits do nanocarriers offer? *Nanomedicine*. 2017;12(6):683-702. [CrossRef]
- [4] Vaishya RD, Khurana V, Patel S, Mitra AK. Controlled ocular drug delivery with nanomicelles. *Wiley Interdisciplinary Reviews: Nanomedicine and Nanobiotechnology*. 2014;6(5):422-37. [CrossRef]
- [5] Srividya B, Cardoza RM, Amin P. Sustained ophthalmic delivery of ofloxacin from a pH triggered *in situ* gelling system. *Journal of controlled release*. 2001;73(2-3):205-11. [CrossRef]
- [6] Liu Z, Li J, Nie S, Liu H, Ding P, Pan W. Study of an alginate/HPMC-based *in situ* gelling ophthalmic delivery system for gatifloxacin. *International journal of pharmaceutics*. 2006;315(1-2):12-7. [CrossRef]
- [7] Wei G, Xu H, Ding PT, Zheng JM. Thermosetting gels with modulated gelation temperature for ophthalmic use: the rheological and gamma scintigraphic studies. *Journal of Controlled Release*. 2002;83(1):65-74. [CrossRef]
- [8] Almeida H, Amaral MH, Lobão P, Lobo JMS. *In situ* gelling systems: a strategy to improve the bioavailability of ophthalmic pharmaceutical formulations. *Drug discovery today*. 2014;19(4):400-12. [CrossRef]
- [9] Dumortier G, Grossiord JL, Agnely F, Chaumeil JC. A review of poloxamer 407 pharmaceutical and pharmacological characteristics. *Pharmaceutical research*. 2006;23(12):2709-28. [CrossRef]
- [10] Muxika A, Etxabide A, Uranga J, Guerrero P, De La Caba K. Chitosan as a bioactive polymer: Processing, properties and applications. *International Journal of Biological Macromolecules*. 2017;105:1358-68. [CrossRef]

- [11] Fazel Nabavi S, Thiagarajan R, Rastrelli L, Daglia M, Sobarzo-Sanchez E, Alinezhad H, Nabavi SM. Curcumin: a natural product for diabetes and its complications. *Current topics in medicinal chemistry*. 2015;15(23):2445-55. [\[CrossRef\]](#)
- [12] Lou J, Hu W, Tian R, Zhang H, Jia Y, Zhang J, Zhang L. Optimization and evaluation of a thermoresponsive ophthalmic *in situ* gel containing curcumin-loaded albumin nanoparticles. *International journal of nanomedicine*. 2014;9:2517. [\[CrossRef\]](#)
- [13] Xie P, Zhang W, Yuan S, Chen Z, Yang Q, Yuan D, Wang F, Liu QH. Suppression of experimental choroidal neovascularization by curcumin in mice. *PloS one*. 2012;7(12):e53329. [\[CrossRef\]](#)
- [14] Pradhan N, Guha R, Chowdhury S, Nandi S, Konar A, Hazra S. Curcumin nanoparticles inhibit corneal neovascularization. *Journal of Molecular Medicine*. 2015;93(10):1095-106. [\[CrossRef\]](#)
- [15] Pescosolido N, Giannotti R, Plateroti AM, Pascarella A, Nebbioso M. Curcumin: therapeutical potential in ophthalmology. *Planta medica*. 2014;80(04):249-54. [\[CrossRef\]](#)
- [16] Ma X, Zhao Y. Biomedical applications of supramolecular systems based on host-guest interactions. *Chemical reviews*. 2015;115(15):7794-839. [\[CrossRef\]](#)
- [17] Trapani A, Lopodota A, Franco M, Cioffi N, Ieva E, Garcia-Fuentes M, Alonso MJ. A comparative study of chitosan and chitosan/cyclodextrin nanoparticles as potential carriers for the oral delivery of small peptides. *European Journal of Pharmaceutics and Biopharmaceutics*. 2010;75(1):26-32. [\[CrossRef\]](#)
- [18] Qiu N, Li X, Liu J. Application of cyclodextrins in cancer treatment. *Journal of Inclusion Phenomena and Macrocyclic Chemistry*. 2017;89(3-4):229-46. [\[CrossRef\]](#)
- [19] Polat HK, Pehlivan SB, Özkul C, Çalamak S, Öztürk N, Aytekin E, Firat A, Ulubayram K, Kocabeyoglu S, Irkeç M, Çalış S. Development of besifloxacin HCl loaded nanofibrous ocular inserts for the treatment of bacterial keratitis: *In vitro*, *ex vivo* and *in vivo* evaluation. *International journal of pharmaceutics*. 2020;585:119552. [\[CrossRef\]](#)
- [20] Zuorro A, Fidaleo M, Lavecchia R. Solubility Enhancement and Antibacterial Activity of Chloramphenicol Included in Modified  $\beta$ -Cyclodextrins. *Bulletin of the Korean Chemical Society*. 2010;31(11):3460-2. [\[CrossRef\]](#)
- [21] Loftsson T, Brewster ME. Pharmaceutical applications of cyclodextrins: basic science and product development. *Journal of pharmacy and pharmacology*. 2010;62(11):1607-21. [\[CrossRef\]](#)
- [22] Rodriguez-Aller M, Guinchard S, Guillarme D, Pupier M, Jeannerat D, Rivara-Minten E, Veuthey JL, Gurny R. New prostaglandin analog formulation for glaucoma treatment containing cyclodextrins for improved stability, solubility and ocular tolerance. *European Journal of Pharmaceutics and Biopharmaceutics*. 2015;95:203-14. [\[CrossRef\]](#)
- [23] Nabih Maria D, Mishra SR, Wang L, Abd-Elgawad A-EH, Soliman OA-E, El-Dahan MS, Jablonski MM. Water-soluble complex of curcumin with cyclodextrins: enhanced physical properties for ocular drug delivery. *Current Drug Delivery*. 2017;14(6):875-86. [\[CrossRef\]](#)
- [24] Mangolim CS, Moriwaki C, Nogueira AC, Sato F, Baesso ML, Neto AM, Matioli G. Curcumin- $\beta$ -cyclodextrin inclusion complex: Stability, solubility, characterisation by FT-IR, FT-Raman, X-ray diffraction and photoacoustic spectroscopy, and food application. *Food chemistry*. 2014;153:361-70. [\[CrossRef\]](#)
- [25] Chen J, Qin X, Zhong S, Chen S, Su W, Liu Y. Characterization of curcumin/cyclodextrin polymer inclusion complex and investigation on its antioxidant and antiproliferative activities. *Molecules*. 2018;23(5):1179. [\[CrossRef\]](#)
- [26] Rojas-Mena AR, López-González H, Rojas-Hernández A. Preparation and characterization of holmium-beta-cyclodextrin complex. *Advances in Materials Physics and Chemistry*. 2015;5(03):87. [\[CrossRef\]](#)
- [27] Van Nong H, Hung LX, Thang PN, Chinh VD, Vu LV, Dung PT, Van Trung T, Nga PT. Fabrication and vibration characterization of curcumin extracted from turmeric (*Curcuma longa*) rhizomes of the northern Vietnam. *SpringerPlus*. 2016;5(1):1-9. [\[CrossRef\]](#)
- [28] Denadai AM, Santoro MM, Lopes MT, Chenna A, de Sousa FB, Avelar GM, Gomes MRT, Guzman F, Salas CE, Sinisterra RD. A supramolecular complex between proteinases and  $\beta$ -cyclodextrin that preserves enzymatic activity. *Biodrugs*. 2006;20(5):283-91. [\[CrossRef\]](#)
- [29] Mashaqbeh H, Obaidat R, Al-Shar'i N. Evaluation and Characterization of Curcumin- $\beta$ -Cyclodextrin and Cyclodextrin-Based Nanosponge Inclusion Complexation. *Polymers*. 2021;13(23):4073. [\[CrossRef\]](#)
- [30] Gaudana R, Jwala J, Boddu SH, Mitra AK. Recent perspectives in ocular drug delivery. *Pharmaceutical research*. 2009;26(5):1197-216. [\[CrossRef\]](#)

- [31] Lumry WR. A review of the preclinical and clinical data of newer intranasal steroids used in the treatment of allergic rhinitis. *Journal of allergy and clinical immunology*. 1999;104(4):s150-s9. [[CrossRef](#)]
- [32] Singh R, Tønnesen HH, Vogensen SB, Loftsson T, Másson M. Studies of curcumin and curcuminoids. XXXVI. The stoichiometry and complexation constants of cyclodextrin complexes as determined by the phase-solubility method and UV-Vis titration. *Journal of inclusion phenomena and macrocyclic chemistry*. 2010;66(3):335-48. [[CrossRef](#)]
- [33] Pramanik A, Sahoo RN, Nanda A, Mohapatra R, Singh R, Mallick S. Ocular permeation and sustained anti-inflammatory activity of dexamethasone from kaolin nanodispersion hydrogel system. *Current Eye Research*. 2018;43(6):828-38. [[CrossRef](#)]
- [34] Bohorquez M, Koch C, Trygstad T, Pandit N. A study of the temperature-dependent micellization of pluronic F127. *Journal of colloid and interface science*. 1999;216(1):34-40. [[CrossRef](#)]
- [35] Okur NÜ, Yozgatli V, Okur ME. In vitro-in vivo evaluation of tetrahydrozoline-loaded ocular *in situ* gels on rabbits for allergic conjunctivitis management. *Drug Development Research*. 2020;81(6):716-27. [[CrossRef](#)]
- [36] Çulcu Ö, Tunçel E, TAMER Sİ, TIRNAKSIZ FF. Characterization of Thermosensitive Gels for the Sustained Delivery of Dexketoprofen Trometamol for Dermal Applications. *Journal of Gazi University Health Sciences Institute*. 2020;2(2):1-12.
- [37] Aderibigbe BA. *In situ*-based gels for nose to brain delivery for the treatment of neurological diseases. *Pharmaceutics*. 2018;10(2):40. [[CrossRef](#)]
- [38] Destruel P-L, Zeng N, Brignole-Baudouin F, Douat S, Seguin J, Olivier E, Dutot M, Rat P, Dufay S, Dufay-Wojcicki A, Maury M, Mignet N, Boudy V. *In situ* gelling ophthalmic drug delivery system for the optimization of diagnostic and preoperative mydriasis: *in vitro* drug release, cytotoxicity and mydriasis pharmacodynamics. *Pharmaceutics*. 2020;12(4):360. [[CrossRef](#)]
- [39] Zhang Y, Huo M, Zhou J, Zou A, Li W, Yao C, Xie S. DDSolver: an add-in program for modeling and comparison of drug dissolution profiles. *AAPS J*. 2010;12(3):263-71. [[CrossRef](#)]
- [40] Virto MR, Elorza B, Torrado S, Elorza MdLA, Frutos G. Improvement of gentamicin poly (D, L-lactic-co-glycolic acid) microspheres for treatment of osteomyelitis induced by orthopedic procedures. *Biomaterials*. 2007;28(5):877-85. [[CrossRef](#)]
- [41] Li N, Wang N, Wu T, Qiu C, Wang X, Jiang S, Zhang Z, Liu T, Wei C, Wang T. Preparation of curcumin-hydroxypropyl- $\beta$ -cyclodextrin inclusion complex by cosolvency-lyophilization procedure to enhance oral bioavailability of the drug. *Drug Development and Industrial Pharmacy*. 2018;44(12):1966-74. [[CrossRef](#)]
- [42] Higuchi T. A phase solubility technique. *Adv Anal Chem Instrum*. 1965;4:117-211.
- [43] Loftsson T, Hreinsdóttir D, Másson M. Evaluation of cyclodextrin solubilization of drugs. *International journal of pharmaceutics*. 2005;302(1-2):18-28. [[CrossRef](#)]
- [44] Waslidge NB, Hayes DJ. A colorimetric method for the determination of lipoxygenase activity suitable for use in a high throughput assay format. *Analytical biochemistry*. 1995;231(2):354-8. [[CrossRef](#)]
- [45] Chung LY, Soo WK, Chan KY, Mustafa MR, Goh SH, Imiyabir Z. Lipoxygenase inhibiting activity of some Malaysian plants. *Pharmaceutical Biology*. 2009;47(12):1142-8. [[CrossRef](#)]
- [46] Re R, Pellegrini N, Proteggente A, Pannala A, Yang M, Rice-Evans C. Antioxidant activity applying an improved ABTS radical cation decolorization assay. *Free radical biology and medicine*. 1999;26(9-10):1231-7. [[CrossRef](#)]
- [47] El-Kamel A. *In vitro* and *in vivo* evaluation of Pluronic F127-based ocular delivery system for timolol maleate. *International journal of pharmaceutics*. 2002;241(1):47-55. [[CrossRef](#)]
- [48] Gupta H, Jain S, Mathur R, Mishra P, Mishra AK, Velpandian T. Sustained ocular drug delivery from a temperature and pH triggered novel *in situ* gel system. *Drug delivery*. 2007;14(8):507-15. [[CrossRef](#)]
- [49] Karatas A, Sonakin O, Kilicarslan M, Baykara T. Poly ( $\epsilon$ -caprolactone) microparticles containing levobunolol HCl prepared by a multiple emulsion (W/O/W) solvent evaporation technique: Effects of some formulation parameters on microparticle characteristics. *Journal of microencapsulation*. 2009;26(1):63-74. [[CrossRef](#)]
- [50] Gamal A, Saeed H, El-Ela FIA, Salem HF. Improving the antitumor activity and bioavailability of sonidegib for the treatment of skin cancer. *Pharmaceutics*. 2021;13(10):1560. [[CrossRef](#)]
- [51] Murtaza G, Ahmad M, Khan SA, Hussain I. Evaluation of cefixime-loaded chitosan microspheres: Analysis of dissolution data using DDSolver. *Dissolution Technologies*. 2012;19(2):13-9. [[CrossRef](#)]

- [52] FDA U. Guidance for Industry: Dissolution testing of immediate-release solid oral dosage forms. Food and Drug Administration, Center for Drug Evaluation and Research (CDER). 1997:1-11.
- [53] Aldeek F, McCutcheon N, Smith C, Miller JH, Danielson TL. Dissolution Testing of Nicotine Release from OTDN Pouches: Product Characterization and Product-to-Product Comparison. *Separations*. 2021;8(1):7. [\[CrossRef\]](#)
- [54] Puthli S, Vavia PR. Stability studies of microparticulate system with piroxicam as model drug. *Aaps Pharmscitech*. 2009;10(3):872-80. [\[CrossRef\]](#)

This is an open access article which is publicly available on our journal's website under Institutional Repository at <http://dspace.marmara.edu.tr>.